Progress In Electromagnetics Research M, Vol. 81, 159–165, 2019

Scintillation Effects in the Magnetized Plasma

George Jandieri[1, *], Akira Ishimaru[2], Jaromir Pistora[1], and Michal Lesnak[1]

Abstract—Statistical characteristics of scattered electromagnetic waves in the turbulent magnetized plasma caused by electron density fluctuations are calculated using complex geometrical optics approximation taking into account both diffraction effects and polarization coefficients. Scintillation level normalized on the variance of the phase fluctuations is analyzed analytically and numerically for small-scale plasma irregularities using the experimental data. New properties of the electromagnetic wave scintillations have been revealed. It is shown that splashes arise in the ionosphere leading to the turbulence and generation of new oscillations (waves and/or Pc pulsations) propagating in space and the terrestrial atmosphere. Turbulence extending in the lower atmospheric layers can influence on the meteorological parameters leading to climate change.

1. INTRODUCTION

Ionospheric scintillation study is one of the important problems of the formation of ionospheric plasma-density irregularities and in space communication. The phenomenon referred to the scintillation of radio signal in the ionosphere was well studied and widely described in the scientific literature [1–3]. Plasma irregularities cause random modulation of the wave front of an incident signal giving rise random phase-modulation of a transmitted wavefront that effects the signal phase and amplitude, polarization, and angle of arrival. Ionospheric scintillation models contain the worldwide climatology of the ionospheric plasma density irregularities that cause scintillation.

The presence of the geomagnetic field leads to the birefringence and anisotropy. Ionospheric irregularities have typical spatial dimensions ranging from several kilometers to few meters, are mainly field-aligned and causing scintillation. Scintillation effects of scattered ordinary and extraordinary waves in the ionospheric plasma for both power-law and anisotropic Gaussian correlation functions of electron density fluctuations have been investigated in [4–7].

The second-order statistical moments are calculated in this paper using the complex geometrical optics approximation taking into account polarization coefficients of both ordinary and extraordinary waves and diffraction effects. Numerical calculations are carried out for small-scale ionospheric plasma irregularities using anisotropic Gaussian 3D spectral function containing both anisotropy factor and slope angle of elongated plasma irregularities with respect to the lines of forces of the geomagnetic field. Scintillation level is estimated in three zones: the non-fully developed diffraction pattern, the fully developed pattern and in the transition area connecting these two regions. Numerical calculations are based on experimental data.

2. FORMULATION

Wave equation for the electric field in the collision magnetized plasma

$$\left(\nabla_i \nabla_j - \Delta\delta_{ij} - k_0^2 \varepsilon_{ij}(\mathbf{r})\right) \mathbf{E_j}(\mathbf{r}) = 0, \tag{1}$$

Received 15 April 2019, Accepted 29 May 2019, Scheduled 11 June 2019

* Corresponding author: George Jandieri (georgejandieri7@gmail.com).

[1] Nanotechnology Centre, VSB-Technical University of Ostrava, Ostrava-Poruba, Czech Republic. [2] Department of Electrical Engineering, University of Washington, FT-10 Seattle, Washington 98 195, USA.

contains components of the second-order permittivity tensor [8]:

$$\begin{aligned}&\varepsilon_{xx}=1-\Delta g,\quad \varepsilon_{xy}=-\varepsilon_{yx}=i\Delta\sqrt{u_L},\quad \varepsilon_{xz}=-\varepsilon_{zx}=-i\Delta\sqrt{u_T},\quad \varepsilon_{yy}=1-\Delta\left(g^2-u_T\right)/g,\\&\varepsilon_{yz}=\varepsilon_{zy}=\Delta ug\sqrt{u_Lu_T},\quad \varepsilon_{zz}=1-\Delta g\left(g^2-u_L\right),\end{aligned}\tag{2}$$

where $\Delta=v/(g^2-u)$, $u_L=u\cos^2\alpha$, $u_T=u\sin^2\alpha$, $\omega_p(\mathbf{r})=[4\pi N(\mathbf{r})e^2/m]^{1/2}$ is the plasma frequency; $u(\mathbf{r})=(eH_0/mc\omega)^2$ and $v(\mathbf{r})=\omega_p^2(\mathbf{r})/\omega^2$ are the magneto-ionic parameters; $N(\mathbf{r})$ is the electron density; e and m are the charge and the mass of electron, respectively; $g=1-is$, $s=\nu_{eff}/\omega$, $\nu_{eff}=\nu_{ei}+\nu_{en}$ is the effective collision frequency of electrons with other plasma particles; α is the angle between the Z-axis (the direction of the wave propagation) and the ambient geomagnetic field $\mathbf{H}_0$ in the yz-plane. Ionospheric structures smaller than the first Fresnel scale $\sqrt{\lambda L}$ (where λ represents the signal wavelength, and L is the distance between the irregular layer and the observation points) imparts both phase and amplitude modulations of the wavefront undergoing refraction or diffraction [9]. We introduce diffraction parameter $\mu=k_\perp/k_0$ [10].

For the solution of Equation (1) we use the complex geometrical optics approximation representing the wave field as $E_j(\mathbf{r})=E_{0j}\exp\{\Phi(\mathbf{r})\}$, where $\Phi(\mathbf{r})$ is the complex phase, $\Phi(\mathbf{r})=\varphi_0+\varphi_1(\mathbf{r})$, $\varphi_0=ik_0x+ik_\perp y$ ($k_\perp\ll k_0$), $\varphi_1(\mathbf{r})$ is a random function of the spatial coordinates.

Applying the modified smooth perturbation method [11, 12] correlation function of the phase fluctuations of a scattered electromagnetic wave caused by the electron density fluctuations in the high-latitude polar ionospheric region is:

$$W_\varphi(\boldsymbol{\eta},L)=\frac{\pi}{2}k_0^4L\Upsilon_0^2\int\limits_{-\infty}^{\infty}dx\int\limits_{-\infty}^{\infty}dyV_n\left\{x,y,-\left[(\mu+y)y+T_0x^2+sT_1x\right]\right\}\exp(-i\eta_xx-i\eta_yy),\tag{3}$$

where η_y and η_x are the nondimensional distances between observation points spaced apart in the principle and perpendicular planes, respectively; $x=k_x/k_0$, $y=k_y/k_0$, $T_1=2P_j'(\mu+y)+\Gamma_j'\left[2(1+\mu y)+y^2\right]$, $T_0=\Gamma_j''\left[\Gamma_j''-P_j''(\mu+y)\right]$, $V_n(x,y)$ is the arbitrary 3D spatial spectrum of electron density fluctuations; the asterisk indicates the complex conjugate; Υ_0^2 should be calculated for a given altitude of the terrestrial ionosphere, and polarization coefficients can be easily calculated in a zero-order approximation containing the magneto-ionic parameters [8]

$$\begin{aligned}\frac{\langle E_y\rangle}{\langle E_x\rangle}&=-i\frac{2\sqrt{u_L}(g-v)}{u_T\mp\sqrt{u_T^2+4u_L^2(g-v)^2}}=-iP_j''-sP_j',\\\frac{\langle E_z\rangle}{\langle E_x\rangle}&=-i\frac{v\sqrt{u_T}\left(g+\sqrt{u_L}P_j\right)}{gu-g^2(g-v)-vu_L}=i\Gamma_j''+s\Gamma_j',\end{aligned}\tag{4}$$

upper sign (index 1) corresponds to the ordinary wave and the lower sign (index 2) to the extraordinary wave.

The variance of the phase fluctuations is [11].

$$\left\langle\varphi_1^2\right\rangle=\frac{\pi}{2}k_0^4L\Upsilon_0^2\int\limits_{-\infty}^{\infty}dx\int\limits_{-\infty}^{\infty}dyV_n(i\Omega_1-\Omega_2),\tag{5}$$

where $\Omega_1=\Gamma_j''\left[\Gamma_j''-P_j''(\mu+y)\right]$, $\Omega_2=2P_j'(\mu+y)+\Gamma_j'\left[2(1+\mu y)+y^2\right]$.

The standard relationship for the weak scattering between the scintillation level S_4 and the 2D phase spectrum describing 2D diffraction pattern on the ground is [13]:

$$S_4^2=2\int\limits_{-\infty}^{\infty}dx\int\limits_{-\infty}^{\infty}dyW_\varphi(x,y)\sin^2\left(\frac{x^2+y^2}{\Xi_f^2}\right),\tag{6}$$

where $\Xi_f=k_f/k_0\equiv\sqrt{4\pi/\lambda L}/k_0$ is the nondimensional Fresnel wavenumber. The double integral in the wave number space does not depend on the shape of the fluctuation spectrum and does not depend on

the intensity fluctuations. The sinusoidal term is responsible for oscillations in the scintillation spectrum. Phase scintillations are usually observed as a phase difference spaced apart receiving antennas or radar systems.

If "frozen-in" plasma irregularities move relative to the receiver or the satellite, the 3D spectral function can be transformed into a one-dimensional spectrum. We assume that irregularities drift transverse to the line of the sight path of the radio signals in the x-axis with the velocity V_x. The power spectrum $P_S(\nu, L)$ is computed from the correlation function of the phase fluctuations [14]:

$$P_\varphi(\nu) = \frac{2\pi}{k_0 V_x} \int_0^\infty dx W_\varphi \left(x = \frac{2\pi\nu}{k_0 V_x},\, y \right), \quad P_S(\nu) = 4P_\varphi(\nu) \sin^2 \left(\frac{\nu}{\nu_f} \right)^2. \tag{7}$$

The Fresnel frequency $\nu_f = V_x/(\pi\lambda L)^{1/2}$ is directly proportional to the drift velocity V_x of plasma irregularities normal to the yz-plane and inversely proportional to the Fresnel radius, and ν is the scintillation frequency.

The standard relationship for weak scattering between the 2D scintillation spectrum $P_S(x, y)$ and the 2D phase correlation function is given by:

$$P_S(x, y) = 4W_\varphi(x, y) \sin^2 \left(\frac{x^2 + y^2}{\Xi_f^2} \right), \tag{8}$$

Equations (7) and (8) describe 2D diffraction patterns at the ground illustrating the strong attenuation of the interference pattern.

3. NUMERICAL CALCULATIONS

The incident electromagnetic wave has a frequency of 3 MHz ($k_0 = 6.28 \cdot 10^{-2}\,\mathrm{m}^{-1}$). Plasma parameters at an altitude of 300 km are $u = 0.22$, $v = 0.28$. The Fresnel radius and Fresnel wavenumber are equal to 5.5 km and $0.64\,\mathrm{km}^{-1}$, respectively.

The distribution of nighttime irregularities which produce satellite scintillation has been examined for a midlatitude location using a large array of receivers [15]. The orientation of the axis of elongation, and movements perpendicular to this axis were measured. It was shown that the irregularities are aligned along the earth's magnetic field in the F-region with observable structures as small as a few hundred meters.

The Gadanki MST radar observations made during the SAFAR ("Study on Atmospheric Forcing And Responses") program show that plasma irregularities with scale sizes ranging from a few centimeters to a few hundred of kilometers are generated [16] due to the Rayleigh-Taylor instability. In Equinox, they are observed as plume structures, while in summer, they are observed as horizontally stratified structures. Below 350 km (where the buoyancy force to the plasma bubble motion can be neglected) the irregularity drift perpendicular to the magnetic field with the velocities 10–100 ms^{-1} and occasionally as high as $300\,\mathrm{ms}^{-1}$.

Numerical calculations are carried out for the anisotropic Gaussian 3D spectral correlation function of the electron density fluctuations. The anisotropic 3D Gaussian spectral function has the following form [17]:

$$W_n(\mathbf{k}) = \frac{\sigma_n^2 l_{||}^3}{8\pi^{3/2}\chi^2} \exp\left(-\frac{k_x^2 l_{||}^2}{4\chi^2} - p_1 \frac{k_y^2 l_{||}^2}{4} - p_2 \frac{k_z^2 l_{||}^2}{4} - p_3 k_y k_z l_{||}^2 \right), \tag{9}$$

where σ_n^2 is the mean-square fractional deviation of electron density. This spectral function contains the anisotropy factor $\chi = l_{||}/l_\perp$ (the ratio of longitudinal and transverse linear sizes of ionospheric plasma irregularities) and the inclination angle γ_0 of elongated irregularities with respect to the magnetic lines of forces; $p_1 = (\sin^2\gamma_0 + \chi^2\cos^2\gamma_0)^{-1}\left[1 + (1-\chi^2)^2 \sin^2\gamma_0 \cos^2\gamma_0/\chi^2\right]$, $p_2 = (\sin^2\gamma_0 + \chi^2\cos^2\gamma_0)/\chi^2$, $p_3 = (1-\chi^2)\sin\gamma_0\cos\gamma_0/2\,\chi^2$. Ellipsoidal shape of the plasma irregularities is caused due by the diffusion processes in the terrestrial ionosphere.

By substituting (9) into Equations (5)–(7) and using the saddle-point method we obtain:

$$S_* = \frac{\int\limits_{-\infty}^{\infty} dy \left[1-\cos(\Upsilon y^2)\right]\cdot \exp\left(-\frac{\xi^2}{4}\Theta_3\right)}{\int\limits_{-\infty}^{\infty} dy \exp\left(-\frac{\xi^2}{4}\Theta_5 y^2\right)}. \tag{10}$$

$$P_{\varphi}^{(\perp)}(\nu) = \frac{G_0}{\nu_0}\exp(-i\eta_x\nu_*)\int\limits_{-\infty}^{\infty} dy \exp\left\{-\frac{\xi^2}{4}\left[\left(\frac{p_2}{16}\Theta_1^2\nu_*^4+\Theta_2\nu_*^2+\Theta_3\right)+s\Theta_4\left(\frac{p_2}{8}\Theta_1\nu_*^3+g\nu_*\right)\right]\right\}$$
$$\cdot\exp(-i\eta_y y), \tag{11}$$

where: $G_0 = \sigma_n^2\xi^3 k_0 L/16\sqrt{\pi}\chi^2$, $\nu_* = \nu/\nu_0$, $\nu_0 = k_0 V_x/2\pi$, $g = \frac{1}{2}p_2\mu - p_3 y + \frac{1}{4}p_2 y^2$, $\Theta_1 = \Gamma_j''\left[\Gamma_j'' - \mathrm{P}_j''(y+\mu)\right]$, $\Theta_2 = \frac{1}{\chi^2} + g\Theta_1$, $\Theta_3 = \frac{p_2}{4}y^4 + (p_2\mu - 2p_3)y^3 + (p_1 + p_2\mu^2 - 4p_3\mu)y^2$, $\Theta_4 = 2\left[\Gamma_j' - \mathrm{P}_j'\mu + (\Gamma_j'\mu - \mathrm{P}_j')y\right] + \Gamma_j' y^2$, $\Theta_5 = p_1 + p_2\mu^2 + 4\,p_3\mu$.

Figures illustrate log-log plots of the normalized scintillation level $S_* = S_4/\sqrt{\langle\varphi_1^2\rangle}$ versus parameter $\Upsilon = 2k_0^2/k_f^2$ for the anisotropic Gaussian irregularities in the magnetized collision plasma at different χ and γ_0 parameters. Left asymptotic area $\Upsilon \ll 1$ (first region) is associated with a significant filtering, non-fully developed diffraction pattern, $\Upsilon \gg 1$ (third region) corresponds to the fully developed pattern. The shaded area (second region) is the transition region between these two regions. In all the figures the diffraction parameter $\mu = 0.08$, curve 1 corresponds: $\chi = 10$, $\gamma_0 = 5°$; curve 2: $\chi = 10$, $\gamma_0 = 10°$; curve 3: $\chi = 20$, $\gamma_0 = 20°$; curve 4: $\chi = 30$, $\gamma_0 = 20°$. The scintillation index depends strongly on the distance between the interferometer elements and characteristic linear scale of plasma irregularities.

Figure 1 depicts log-log plots of the normalized scintillation level at $\xi = 80$ ($l_{||} = 1.3\,\mathrm{km}$), the distance between observation points: $\eta_x = 5$, $\eta_y = 4$; $s = 0.01$. For the curve 3, no oscillations are in the transient zone and arise only in the fully-developed diffraction region; four minimums are in the normalized scintillation level S_*: $\Upsilon = 24$, 47, 72 and 95. The curve 4 has 15 minimums. All minimums satisfy the relationship: $1:2:3:4$.... In this case, oscillations are not observed for the curves 1 and 2.

Decreasing the anisotropy factor $\xi = 60$ ($l_{||} = 950\,\mathrm{m}$) (Figure 2), $\eta_x = 3$, $\eta_y = 3$; $s = 10^{-3}$ scintillation arising in a transient region is increased in the fully-developed diffraction area (curves 3 and 4). Minimums S_* are at the same points as in the previous case.

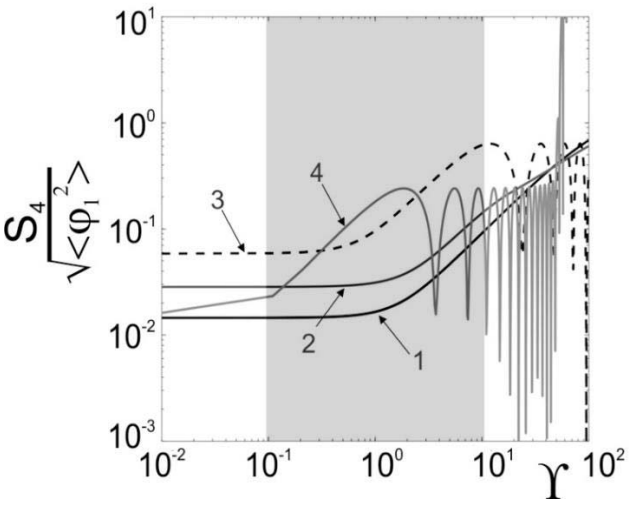

Figure 1. Scintillation level S_* versus parameter Υ at $\xi = 80$, $\chi = 10 \div 30$, $\gamma_0 = 5° \div 20°$.

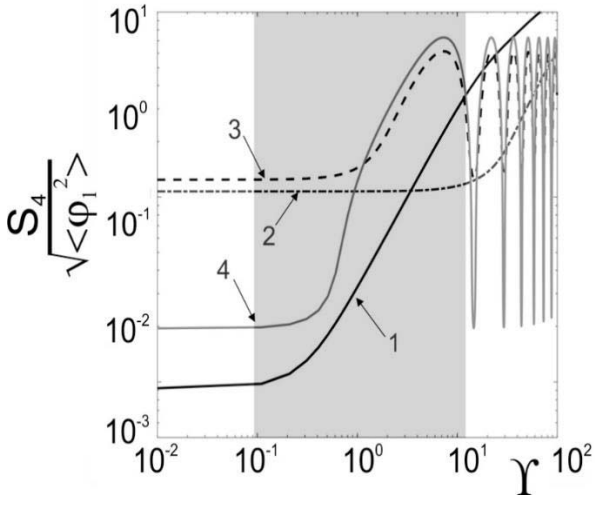

Figure 2. Scintillation level S_* versus parameter Υ at $\xi = 60$, $\chi = 10 \div 30$, $\gamma_0 = 5° \div 20°$.

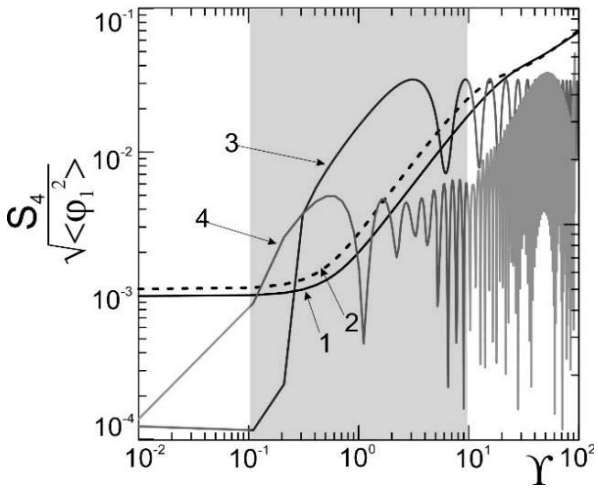

Figure 3. Normalized scintillation spectrum S_* versus parameter Υ for 3 MHz incident EM wave; Curve 1 corresponds to the isotropic case ($\chi = 10$, $\gamma_0 = 5°$), curve 2 ($\chi = 10$, $\gamma_0 = 10°$), curve 3 ($\chi = 20$, $\gamma_0 = 20°$), curve 4 ($\chi = 30$, $\gamma_0 = 20°$).

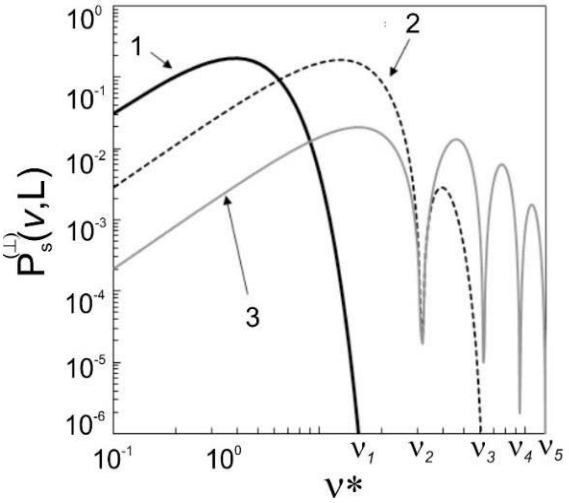

Figure 4. Power spectrum of the intensity fluctuations for the extraordinary wave. Curve 1 corresponds to the isotropic case $\chi = 1$ and $\gamma_0 = 0°$, curve 2 depicts $\chi = 5$ and $\gamma_0 = 5°$, curve 3: $\chi = 15$ and $\gamma_0 = 10°$.

Figure 3 illustrates the log-log plots of the normalized scintillation spectrum S_* versus parameter Υ at $\xi = 10(l_{||} \approx 160\,\text{m})$, $\eta_x = 5$ and $\eta_y = 2$. Since $\Upsilon = 8$ powerful splashes arise in the energetic spectrum transforming their energy into plasma turbulence increasing its intensity. Turbulence has an influence on the meteorological parameters in the lower atmospheric layers leading to climate change. Harmonic oscillations are generated in a transient zone due to the collision between the plasma particles propagating in the terrestrial atmosphere and space as new electromagnetic waves and/or geomagnetic Pc pulsations (see Table 1).

Knowledge of speed of the movement of ionospheric plasma irregularities allows to calculate the power spectrum containing the Fresnel frequency $\nu_f = V/(\pi\lambda L)^{1/2}$ and sinusoidal term responsible

Table 1.

χ	γ_0 (in degrees)	Υ	k_f (m^{-1})	Comments
20	0	8	0.0314	Dumped oscillations
	10	7	0.0336	
	20	6	0.0363	Harmonic oscillations
25	0	4	0.0444	Dumped oscillations
	10	3.5	0.0475	Harmonic oscillations
	20	3.3	0.0489	Nonstationary oscillations (turbulence) until $Y = 40$, after only harmonic oscillations
30	0	2	0.0628	Dumped oscillations
	10	1.9	0.0644	Nonstationary oscillations (turbulence) until $Y = 30$, after harmonic oscillations
	20	1.9	0.0644	Nonstationary oscillations (turbulence)

for oscillations in the scintillation spectrum and calculate the frequencies of the scintillation spectrum. The drift velocity of scattering irregularities embedded in the ionosphere and the characteristic velocity derived with the correlation method (the three-station method) have been considered in [18]. The drift velocity varies in the 84 m/s–102 m/s interval.

Figure 4 depicts the curves of the power spectrum of the intensity fluctuations for the extraordinary wave in the collision magnetized plasma perpendicular to the principal plane at $l_{||} \approx 160$ m, $\eta_x = \eta_y = 5$. Numerical calculations show that for the extraordinary wave first minimum is at $\nu_1 = 1.6$ Hz, next minimums are at: 3.2 Hz, 6.1 Hz, 9,4 Hz, 12.6 Hz, thus satisfying the condition: $1 : 2 : 3 : 4$ and so on. Inflection points are: for the curve 1 at $\nu = 0.5$ Hz; for the curve 2 at $\nu = 2$ Hz and 4 Hz; and for the curve 3 at $\nu = 2$ Hz, 5 Hz, 8 Hz, 11 Hz and 14 Hz. The first minimum for the ordinary wave is at: $\nu_1 = 1.45$ Hz, next minimums are at: 3.2 Hz; 6.3 Hz; 9.4 Hz; 12.9 Hz.

4. CONCLUSION

Second-order statistical moments of scattered electromagnetic wave have been obtained for the arbitrary correlation function of electron density fluctuations using complex geometrical optics approximation taking into account diffraction effects and polarization coefficients. Scintillation level and the power spectrum have been analytically and numerically computed for the anisotropic Gaussian correlation function of anisotropic plasma irregularities containing anisotropy factor and inclination angle with respect to the geomagnetic lines of force. New properties of the electromagnetic wave scintillations have been revealed. Analyses of the normalized scintillation level of scattered radiation for an incident 3 MHz wave show that splashes and turbulence arise in the terrestrial ionosphere. Extending turbulence in the lower atmospheric layers can influence the meteorological parameters causing climate change. Stationary oscillations are generated in the collision magnetized plasma (collision frequency is $s \approx 0.01$) with small-scale plasma irregularities having characteristic spatial scales in the interval 80 m–1.3 km. Scintillation slump is inversely proportional to the anisotropy factor. Minimums of the power spectrum of the intensity fluctuations for the extraordinary wave satisfy the condition: $1 : 2 : 3 : 4$ and so on. The theory should be generalized for conductive anisotropic turbulent media using the same approach as given in this paper.

ACKNOWLEDGMENT

This work was partially supported by the Ministry of Education, Youth and Sports: by the National Program of Sustainability (NPU II) project "IT4 Innovations excellence in science — LQ1602".

REFERENCES

1. Wernik, A. W., J. A. Secan, and E. J. Fremouw, "Ionospheric irregularities and scintillation," *Advances Space Research*, Vol. 31, No. 4, 971–981, 2003.
2. Xu, Z.-W., W. Jian, and Z.-S. Wu, "A survey of ionospheric effects on space-based radar," *Waves in Random Media*, Vol. 14, 189–273, 2004.
3. Aarons, J., "Global morphology of ionospheric scintillation," *Proc. IEEE*, Vol. 70, 360–378, 1982.
4. Jandieri, G. V., A. Ishimaru, V. G. Jandieri, A. G. Khantadze, and Z. M. Diasamidze, "Model computations of angular power spectra for absorptive turbulent magnetized plasma," *Progress In Electromagnetic Research*, Vol. 70, 307–328, 2007.
5. Jandieri, G. V., Z. M. Diasamidze, and M. R. Diasamidze, "Scintillation spectra of scattered electromagnetic waves in turbulent magnetized plasma," *Journal of Basic and Applied Physics*, Vol. 2, No. 4, 224–234, 2013.
6. Jandieri, G., A. Ishimaru, B. Rawat, O. Kharshiladze, and Z. Diasamidze, "Power spectra of ionospheric scintillation," *Advanced Electromagnetics*, Vol. 6, 42–51, 2017.
7. Jandieri, G., A. Ishimaru, B. Rawat, V. G. Gavrilenko, and O. Kharshiladze, "Statistical moments and scintillation level of scattered electromagnetic waves in the magnetized plasma," *Progress In Electromagnetic Research C*, Vol. 84, 11–22, 2018.

8. Ginzburg, V. L., *Propagation of Electromagnetic Waves in Plasma*, Gordon and Beach, New York, 1961.
9. Xu, Z.-W., J. Wu, and Z.-S. Wu, "A survey of ionospheric effects on space-based radar," *Waves in Random Media*, Vol. 14, No. 2, 189–273, 2004.
10. Jandieri, G. V. and A. Ishimaru, "Some peculiarities of the spatial power spectrum of scattered electromagnetic waves in randomly inhomogeneous magnetized plasma with electron density and external magnetic field fluctuations," *Progress In Electromagnetic Research B*, Vol. 50, 77–95, 2013.
11. Jandieri, G. V., ""Double-humped effect" in the turbulent collision magnetized plasma," *Progress In Electromagnetic Research M*, Vol. 48, 95–102, 2016.
12. Jandieri, G. V., A. Ishimaru, B. Rawat, and N. K. Tugushi, "Peculiarities of the spatial power spectrum of scattered electromagnetic waves in the turbulent collision magnetized plasma," *Progress In Electromagnetics Research*, Vol. 152, 137–149, 2015.
13. Rufenach, C. L., "Ionospheric scintillation by a random phase screen: Spectral approach," *Radio Science*, Vol. 10, No. 2, 155–165, 1975.
14. Rufenach, C. L., "Power-law wavenumber spectrum deduced from ionospheric scintillation observations," *Journal of Geophysical Research*, Vol. 77, 4761–4772, 1972.
15. MacDougall, J. W., "Distribution of the irregularities which produce ionospheric scintillations," *J. Atmospheric and Terrestrial Physics*, Vol. 43, No. 4, 317–325, 1981.
16. Patra, A. K. and D. V. Phanikumar, "Intriguing aspects of F-region plasma irregularities revealed by the Gadanki radar observations during the SAFAR campaign," *Ann. Geophys.*, Vol. 27, 3781–3790, 2009.
17. Jandieri, G. V., A. Ishimaru, V. G. Jandieri, A. G. Khantadze, and Z. M. Diasamidze, "Model computations of angular power spectra for anisotropic absorptive turbulent magnetized plasma," *Progress In Electromagnetics Research*, Vol. 70, 307–328, 2007.
18. Burke, M. J., "Validity of three-station methods of determining ionospheric motions," *Journal of Atmospheric and Terrestrial Physics*, Vol. 38, 553–559, 1976.